Snapshot Inversion Recovery: An Optimized Single-Shot T1-weighted Inversion-Recovery Sequence for Improved Fetal Brain Anatomic Delineation[1]

Christina Malamateniou, PhD
Amy K. McGuinness, BSc
Joanna M. Allsop, DCR
Declan P. O'Regan, FRCR, PhD
Mary A. Rutherford, FRCR, MD
Joseph V. Hajnal, PhD

Purpose: To prospectively evaluate the clinical effectiveness of snapshot inversion recovery (SNAPIR), which is a dedicated optimized inversion-recovery-prepared single-shot fast spin-echo T1-weighted sequence, in the delineation of normal fetal brain anatomy compared with that of the currently used T1-weighted gradient-echo protocol, which often yields images of poor quality due to motion artifacts and inadequate contrast.

Materials and Methods: This study was approved by the hospital research ethics committee, and informed written consent was obtained from all patients. Forty-one fetuses were examined at 19–37 weeks gestation (mean, 29 weeks gestation) by using both the standard T1-weighted protocol and the optimized T1-weighted SNAPIR protocol with a 1.5-T imager. Two independent blinded observers performed qualitative analysis, evaluating overall diagnostic quality, detailed anatomic delineation, and severity of motion artifacts. Quantitative analysis comprised calculation of contrast ratios (CRs) for the cortical gray matter, subplate, white matter, and cerebrospinal fluid. The Wilcoxon signed rank test was used to compare image rating scores, the paired *t* test was used to compare CRs, and κ statistics were used to test interobserver agreement.

Results: Both overall diagnostic quality ($P < .001$) and detailed anatomic delineation ($P < .001$) were enhanced with SNAPIR compared with the standard T1-weighted acquisition. Also, motion artifacts were less severe ($P = .008$) and less extensive ($P < .001$) with SNAPIR. Corresponding CRs were increased with SNAPIR in seven of eight examined regions.

Conclusion: SNAPIR is a promising robust alternative to the current T1-weighted acquisitions; its role in the detection of disease requires further study.

Supplemental material: *http://radiology.rsna.org/lookup/suppl/doi:10.1148/radiol.10100381/-/DC1*

[1] From the Robert Steiner MRI Unit, Imaging Sciences Department, Clinical Sciences Centre, Hammersmith Hospital Campus, Imperial College, DuCane Rd, London W12 0HS, England. Received February 17, 2010; revision requested April 6; revision received July 10; accepted July 27; final version accepted August 11. Supported by the Medical Research Council and the Biomedical Research Centre Academic Health Sciences Centre. **Address correspondence to** C.M. (e-mail: *cm1@imperial.ac.uk*).

Magnetic resonance (MR) imaging is an important diagnostic tool with which to assess in vivo brain development. The use of rapid MR sequences is essential for successful fetal imaging in utero, where both maternal motion and fetal motion are present (1).

Currently, T2-weighted single-shot fast spin-echo sequences are the mainstay for fetal brain MR imaging; they generate high-quality and high-contrast images, even in the presence of fetal and maternal motion (2). These fast sequences enable complete filling of the k-space for a single section within one repetition period (3), thereby removing the need for sedation or maternal breath holding (4).

However, the quality of images obtained with commonly used fetal T1-weighted gradient-echo (GRE) breath-hold acquisitions is relatively poor. This is mainly due to artifacts from maternal and fetal motion and inadequate gray-white matter contrast (5). Nevertheless, MR examination of the fetal brain would be incomplete without performance of a T1-weighted sequence to enable one to confirm normal or abnormal anatomy, as well as to identify hemorrhage, fat, or myelination near term (6). Thus, an optimized T1-weighted fetal protocol would considerably advance the diagnosis and further the possibilities for image analysis (7).

Inversion-recovery techniques enhance T1-weighted contrast. The addition of an inversion prepulse to attain good T1 weighting has proved successful in cardiac (8) and abdominal MR protocols (9) in adults and has enabled robust imaging in anatomic regions prone to image degradation due to motion artifacts. Furthermore, the fluid-attenuated inversion-recovery sequence (10) has been used previously to increase T1 contrast in the fetal brain, albeit not in a systematic fashion (11). T1-weighted inversion recovery may also be combined with phase-sensitive reconstruction to improve the dynamic range, as opposed to standard magnitude reconstruction (12).

A dedicated optimized inversion-recovery-prepared single-shot fast spin-echo T1-weighted sequence (hereafter, snapshot inversion recovery [SNAPIR]) for use in fetuses offers a potentially robust alternative to standard fetal T1-weighted GRE imaging (13). The aim of this study was to prospectively evaluate the clinical effectiveness of SNAPIR in the delineation of normal fetal brain anatomy compared with that of the currently used T1-weighted GRE MR imaging protocol in clinical practice (11,14).

Advances in Knowledge

- Snapshot inversion recovery (SNAPIR) can be used to create T1-weighted fetal brain images that delineate fetal brain anatomy better than do standard gradient-echo (GRE) T1-weighted sequences.
- SNAPIR is less sensitive to unpredictable fetal motion compared with standard GRE T1-weighted sequences, resulting in less severe and less extensive motion artifacts.

Implication for Patient Care

- SNAPIR is a robust method with which to obtain T1-weighted data that complement data obtained with T2-weighted acquisitions; therefore, it enables one to perform a more comprehensive MR examination of fetal brain anatomy.

Materials and Methods

Subjects

This study was approved by the hospital research ethics committee, and informed written consent was obtained. We examined 41 pregnant women (median gestational age, 28.57 weeks; gestational age range, 18.86–37 weeks) for the following clinical reasons: fetal brain ventriculomegaly (n = 12), posterior fossa abnormalities (n = 7), intrauterine growth restriction (n = 6), congenital body abnormalities (n = 4), complications of multiple pregnancies (n = 2), and maternal illness (n = 1). Eight of the women examined were healthy volunteers.

Subjects were initially placed in the supine position, feet first, on the imager table so that the obstetrician could detect the fetal head; patients were positioned as close as possible to the isocenter of the imager to maximize the signal-to-noise ratio. Subjects were then rotated approximately 45° from this position to avoid compression of the inferior vena cava and were supported with foam pads to maximize comfort.

Data Acquisition

Examinations were performed with a 1.5-T imager (Achieva; Philips Medical Systems, Best, the Netherlands) with a maximum gradient strength of 31 mT/m and a maximum slew rate of 200 mT/m/msec. A five-element cardiac phased-array surface coil (SENSE-cardiac; Philips Medical Systems) was positioned directly over the fetal head.

Fetuses were examined in the axial plane with the following sequences: *(a)* a standard fetal T1-weighted GRE breath-hold acquisition that was modified from that described in the literature (11,14) to optimize examination time and contrast and *(b)* a T1-weighted SNAPIR acquisition (Table 1). Single-shot fast spin-echo T2-weighted images in all planes were acquired as part of a standard fetal brain MR examination.

Prior to initiation of the study, we optimized the SNAPIR sequence. The

Published online before print
10.1148/radiol.10100381

Radiology 2011; 258:229–235

Abbreviations:
CR = contrast ratio
GRE = gradient echo
SNAPIR = snapshot inversion recovery

Author contributions:
Guarantor of integrity of entire study, M.A.R.; study concepts/study design or data acquisition or data analysis/interpretation, all authors; manuscript drafting or manuscript revision for important intellectual content, all authors; manuscript final version approval, all authors; literature research, C.M., A.K.M., M.A.R.; clinical studies, C.M., A.K.M., J.M.A., M.A.R.; statistical analysis, C.M., D.P.O., J.V.H.; and manuscript editing, C.M., A.K.M., D.P.O., M.A.R., J.V.H.

Potential conflicts of interest are listed at the end of this article.

Table 1

Imaging Parameters Used with Fetal Brain MR Imaging T1-weighted Protocols

Parameter	SNAPIR	T1-weighted GRE
Breath holding	No	Yes
Echo time (msec) (minimum)	8.6	6
Repetition time (msec)	20 000–22 000 (shortest)	142
Inversion time (msec)	400	NA
Field of view (mm)	320 × 340	320 × 300
Resolution (mm)	1 × 1	1.2 × 1.6
Section thickness (mm)	4	6
No. of sections acquired	20	12
Sensitivity-encoding factor	2	None
Half Fourier	No	No
Total acquisition time (sec)	40	17

Note.—NA = not applicable.

optimization process is shown in Figures E1–E4 (online). The optimization process involved testing different parameters for MR imaging data acquisition aspects, such as inversion time, spatial resolution, field of view, reconstruction method, and sensitivity encoding factor. Each test involved at least three patients so that we could confirm the results; none of these patients were included in this validation study.

The inversion time for SNAPIR was set to 400 msec (Fig E1 [online]), which enabled gray-white matter contrast without placing either tissue close to its null point. Longer inversion times were more vulnerable to motion between inversion and readout, increasing vulnerability to artifacts. The voxel size was set to 1 × 1 × 4 mm (Fig E2 [online]) for finer anatomic delineation and adequate signal-to-noise ratio. A field of view of 320 × 340 mm was sufficient to cover the required fetal anatomy over a wide range of gestations (13). A sensitivity encoding factor of 2.00 was used to shorten the imaging time and minimize the occurrence of motion artifacts.

The SNAPIR data were reconstructed by using magnitude and phase-sensitive reconstruction. Given the short inversion time of 400 msec, in which signal intensities of all tissues are negative (Fig E3 [online]), as well as the robustness of the magnitude against the phase errors of the phase-sensitive reconstruction (12), inversion of the magnitude images was used to achieve the desired T1 contrast (Fig E4 [online]).

Analysis

Images were qualitatively assessed by rating diagnostic image quality, motion artifact severity, and motion artifact extent over the total number of sections in all subjects, as well as by performing a more detailed anatomic delineation analysis in 10 subjects. These 10 subjects were selected because their conventional T1-weighted GRE images were of good quality; therefore, biases could be minimized when comparing these images with images obtained with optimized SNAPIR.

Qualitative Analysis

An author (M.A.R., 20 years of experience in MR imaging) performed overall diagnostic quality assessment. Three authors (A.K.M., C.M., and J.V.H.; 5, 7, and 20 years of experience in MR imaging, respectively) assessed artifact severity. Motion artifact severity was based on the difficulty associated with visualization of the underlying anatomy, and it was evaluated on a four-point scale, as follows: 0, no artifact present; 1, mild artifact present (underlying anatomy well visualized); 2, moderate artifact present (underlying anatomy can be visualized but delineation is suboptimal); and 3, severe artifact present (underlying anatomy cannot be visualized). The fraction of sections damaged by motion artifact over the total number of acquired sections was calculated for both imaging protocols to evaluate the extent to which data quality was affected.

Two independent observers (M.A.R., A.K.M.) who were blinded to the acquisition technique performed detailed visual analysis with ImageJ software (National Institutes of Health, *http://rsb.info.nih.gov/ij/*). They used the axial T1-weighted GRE and the SNAPIR inverted magnitude data sets in a subset of 10 patients who were selected because they had the best quality T1-weighted GRE acquisition; this was a representative sample size of the population (gestational age range of population, 19–37 weeks; mean gestational age of population, 29 weeks; gestational age range of subgroup, 22–34 weeks; mean gestational age of subgroup, 28 weeks). Images were evaluated for delineation of 26 normal anatomic structures (Table 2) with the following three-point rating system: 1, uninterpretable (anatomy inadequately defined and/or presence of severe artifact, rendering the image nondiagnostic); 2, suboptimal (well-defined anatomy over the majority of the brain, with some artifacts at presentation; interpretation is possible but not ideal); and 3, good (well-defined anatomy over the entire brain, with no artifact present; comparable with postnatal MR imaging quality).

Quantitative Analysis

An author (A.K.M., 5 years of experience with MR imaging) performed quantitative measurement. This comprised calculation of contrast ratio (CR) with the following equation: $CR = SI_1 - SI_2/\sqrt{(SD_1^2 + SD_2^2)}$, where SI_1 and SI_2 are the mean signal intensities of the different tissues measured in a relatively homogeneous area of the brain and SD_1 and SD_2 are their respective standard deviations. CRs represent a ratio of signal intensities between two different tissues: cortical gray matter (CGM), the subplate (SP), white matter (WM), and cerebrospinal fluid (CSF). CRs were calculated with the following equations: CR_1 = CGM/WM, CR_2 = CGM/SP, CR_3 = WM/SP, and CR_4 = CGM/CSF. Signal intensity was measured by manually

Table 2

Detailed Anatomic Delineation Scores for Two Observers and Two MR Protocols

	Observer 1						Observer 2						
	SNAPIR Score			T1 GRE Score			SNAPIR Score			T1 GRE Score			
Anatomic Structure	1	2	3	1	2	3	1	2	3	1	2	3	*P* Value
Teeth (five buds)	0	7	3	10	0	0	1	6	3	10	0	0	.008
Eyes	0	0	10	0	10	0	0	0	10	1	8	1	.002
Lenses	0	4	6	2	7	1	0	8	2	3	7	0	.008
Optic nerves	3	7	0	5	5	0	4	4	2	7	3	0	.006
Optic chiasm	0	3	7	4	5	1	1	5	4	7	3	0	.004
Pituitary gland	7	3	0	7	2	1	5	4	1	8	1	1	>.999
Skull	1	5	4	3	7	0	0	2	8	1	8	1	.004
Supratentorial extracerebral space	0	0	10	0	10	0	0	0	10	0	5	5	.060
Cisterna magna	0	0	10	1	9	0	0	0	10	1	7	2	.002
Cortical rim and convolutions	0	0	10	0	10	0	0	0	10	0	10	0	.002
White matter and cortex differentiation	0	0	10	0	10	0	0	0	10	1	7	2	.002
Basal ganglia and thalami and white matter differentiation	1	8	1	4	6	0	8	1	1	7	3	0	.297
Periventricular white matter details	0	3	7	4	6	0	1	9	0	8	2	0	.002
Subplate	0	3	7	5	5	0	0	5	5	3	7	0	.002
Germinal matrix	2	8	0	9	1	0	4	6	0	8	2	0	.060
Septum pellucidum	1	2	7	8	2	0	3	2	5	8	1	1	.004
Lateral ventricles	0	0	10	0	10	0	0	1	9	1	9	0	.002
Third ventricle	0	1	9	5	4	1	1	2	7	4	5	1	.004
Fourth ventricle	0	1	9	2	6	2	0	1	9	1	8	1	.008
Aqueduct	1	4	5	8	2	0	2	3	5	8	2	0	.004
Mesencephalon	0	0	10	2	8	0	0	2	8	2	8	0	.002
Pons	0	0	10	3	7	0	1	1	8	2	8	0	.004
Vermis	0	1	9	5	5	0	0	3	7	2	8	0	.004
Cerebellar hemispheres	0	0	10	1	9	0	0	2	8	2	8	0	.002
Dentate nuclei	3	3	4	8	2	0	7	3	0	8	2	0	.156
Myelination	5	5	0	8	2	0	5	4	1	10	0	0	.290

Note.—Unless otherwise indicated, data are numbers of observations per score for each anatomic structure, observer, and MR imaging protocol.

placing regions of interest (minimum coverage, 25 pixels) on a pixel-by-pixel basis over corresponding anatomic areas on T1-weighted GRE images (mean region of interest, 36.59 pixels ± 4.67 [standard deviation]; range, 25–84 pixels) and SNAPIR images (mean region of interest, 25.89 pixels ± 2.94; range, 25–41 pixels) at the temporal lobe and central sulcus levels. We used FSL software (release 4.1; University of Oxford, *http://www.fmrib.ox.ac.uk/fsl/*) (15).

Statistical Analysis

We used the paired *t* test (16) to compare CRs and the fraction of sections damaged by motion artifacts between the two MR acquisitions. We also used the Wilcoxon signed rank test (17,18) to compare image rating scores for overall diagnostic quality, detailed anatomic delineation, and severity of motion artifacts between the two MR acquisitions. A *P* value of less than .05 indicated a significant difference. The *P* values for comparing the two MR acquisitions were based on average scores between the two observers. Interobserver agreement for the detailed visual analysis was evaluated with the Cohen κ coefficient (19) weighted by $W_{ij} = 1-[(i-j)/(k-1)]^2$, where *W* represents weight; *i*, the number of the row; *j*, the number of the column; and *k*, the number of categories used (20). A κ value of 0.00–0.20 indicated poor agreement; a κ value of 0.21–0.40, fair agreement; a κ value of 0.41–0.60, moderate agreement; a κ value of 0.61–0.80, substantial agreement; and a κ value of 0.81–1.0, very good agreement. We used a statistical software package (Statsdirect, version 2.7.7; Statsdirect, Cheshire, England).

Results

Delineation of fetal brain anatomy was enhanced with the SNAPIR protocol compared with that with the T1-weighted GRE protocol (Fig 1), as assessed with both qualitative and quantitative analyses.

Overall diagnostic quality ratings were higher ($P < .001$) for the SNAPIR protocol (mean, 2.40 ± 0.45) than for the T1-weighted GRE protocol (mean, 1.45 ± 0.37). Mean severity of motion artifacts was rated 0.95 ± 0.92 with

Radiology

Figure 1

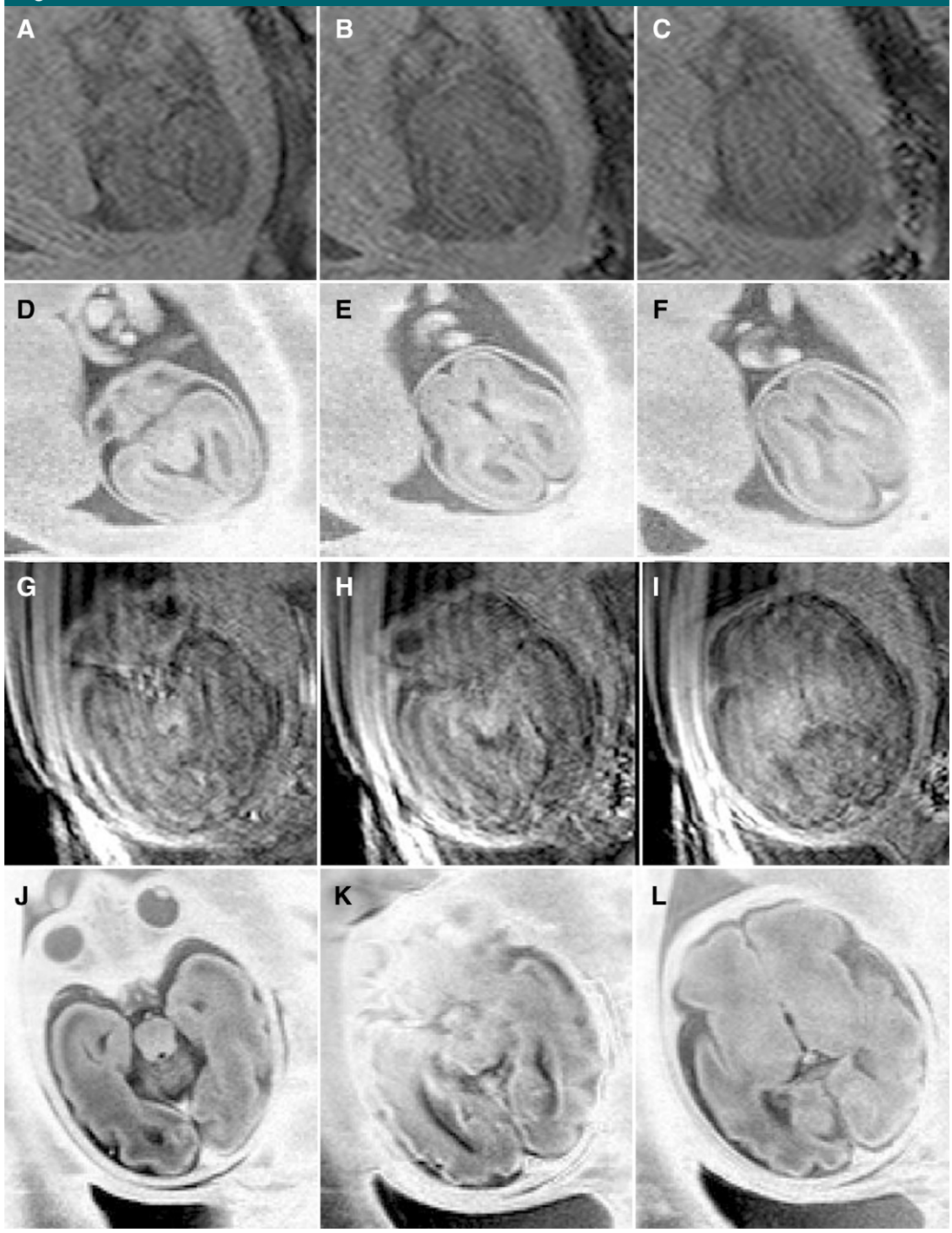

Figure 1: Consecutive axial MR images show a fetus at, *A–F,* 21 weeks gestation and, *G–L,* 32 weeks gestation. Anatomic delineation with SNAPIR at, *D–F*, early and, *J–L*, late gestation was superior to that with the standard T1-weighted GRE breath-hold acquisition at, *A–C*, early and, *G–I*, late gestation. SNAPIR images were also more robust to patient motion, with resulting motion artifacts affecting only isolated sections (*K*) rather than the whole data set, as with the T1-weighted GRE protocol (*G–I*).

Figure 2

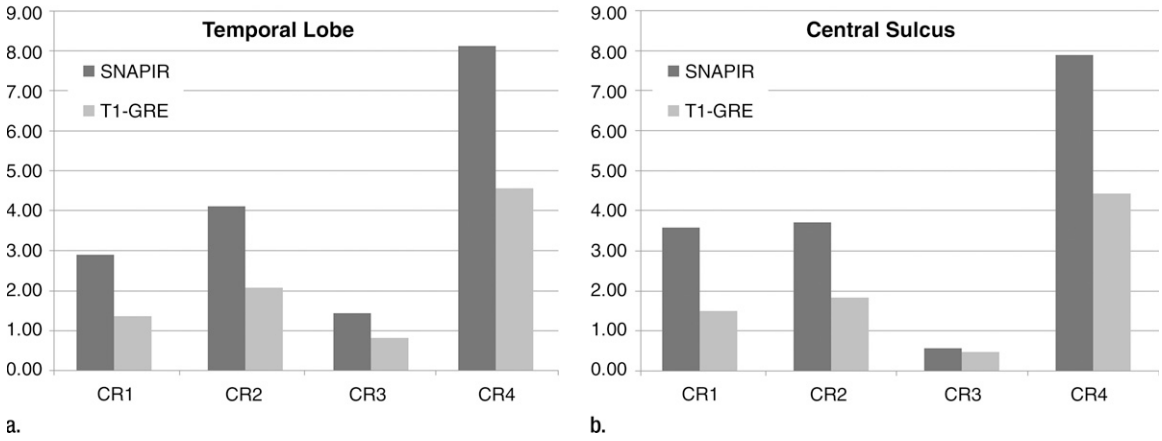

Figure 2: **(a, b)** Graphs show CR differences between the SNAPIR protocol and the T1-weighted GRE protocol at the level of the **(a)** temporal lobe and **(b)** central sulcus. CRs were significantly higher with the SNAPIR protocol than with the T1-weighted GRE protocol at both anatomic levels, with the exception of CR_3 at the anatomic level of the central sulcus.

the SNAPIR protocol and 1.49 ± 0.71 with the T1-weighted GRE protocol ($P = .008$). The mean percentage of sections affected by motion artifacts was only 11% ± 9 with the SNAPIR protocol, whereas it was 77% ± 28 with the T1-weighted GRE protocol ($P < .001$).

The results of detailed visual analysis were again favorable for SNAPIR, with increased depiction of all anatomic structures, based on average rating scores ($P < .001$). More specifically, delineation of the majority of anatomic structures studied (19 of 26 structures) was improved with SNAPIR (Table 2). Interobserver agreement for the detailed visual analysis was very good ($\kappa = 0.87$).

CRs were increased with the SNAPIR protocol at the level of the temporal lobe for CR_1 ($P = .01$), CR_2 ($P = .008$), CR_3 ($P = .03$), and CR_4 ($P = .002$). Similarly, CRs were increased with SNAPIR at the level of the central sulcus for CR_1 ($P < .001$), CR_2 ($P < .001$), and CR_4 ($P = .01$), but not for CR_3 ($P = .64$). The CR differences between the SNAPIR protocol and the T1-weighted GRE sequence in the temporal lobe and at the level of the central sulcus can be seen in Figure 2.

Discussion

Both qualitative and quantitative analysis of the different image data sets revealed delineation of anatomic structures of the fetal brain was significantly improved with the SNAPIR protocol compared with the T1-weighted GRE breath-hold sequence, which is currently considered the mainstay in clinical practice.

The SNAPIR protocol proved more robust to fetal motion. A smaller fraction of SNAPIR images had motion artifacts, with artifacts usually restricted to one or two sections, whereas the effects of motion were generally detrimental with the T1-weighted GRE sequence, resulting in motion artifacts that usually spanned all acquired sections. This was mainly due to the single-shot fast data acquisition mode used in the SNAPIR protocol, which limited the time for motion to occur during readout (3). Another advantage with the SNAPIR protocol was that motion artifacts did not severely affect visualization of the underlying anatomy, as they usually consisted of contrast changes or mild blurring; the opposite was true for motion artifacts encountered with the T1-weighted GRE sequence, where visualization of the underlying fetal brain anatomy was often poor. The SNAPIR protocol does not require breath holding, which is not always well tolerated by pregnant women and which is crucial for acquisition of a successful GRE data set that is devoid of respiratory motion artifacts.

Real reconstruction increases the dynamic range of contrast by estimating and removing the background phase to retrieve the correct polarity information (21); however, it is vulnerable to phase errors, which often require time-consuming and computationally intensive phase-correction postprocessing (12). Thus, in this study, we used the inverted magnitude images, which yielded robust results at no additional time penalty, as they were directly retrieved from the imaging console, without the need for advanced image postprocessing.

The primary limitation of our study was that some centrally located structures were not adequately depicted with the SNAPIR protocol; the opposite was true for peripheral anatomy, such as the cortical rim and convolutions, the depiction of which was superior with the SNAPIR protocol. This might relate to k-space sampling and warrants further investigation. We would also like to test this protocol with a bigger sample size to confirm our results.

The SNAPIR protocol is a promising robust alternative to the currently used T1-weighted GRE sequence; however, its role in the clinical examination of the fetal brain needs to be established with larger-scale studies that focus on its sensitivity in the detection of fetal brain abnormalities in comparison with the sensitivity of standard protocols.

In conclusion, the SNAPIR fetal optimized protocol yields robust T1-weighted images that are suitable for clinical and research applications. This technique holds promise for advancing T1-weighted imaging of the fetal brain in a predominantly T2-weighted field.

Disclosures of Potential Conflicts of Interest: C.M. Financial activities related to the present article: received a grant from Biomedical Research Centre, Academic Health Sciences Center (DCIM P31599). Financial activities not related to the present article: none to disclose. Other relationships: none to disclose. **A.K.M.** No potential conflicts of interest to disclose. **J.M.A.** No potential conflicts of interest to disclose. **D.P.O.** No potential conflicts of interest to disclose. **M.A.R.** No potential conflicts of interest to disclose. **J.V.H.** Financial activities related to the present article: none to disclose. Financial activities not related to the present article: is a board member and has stock/stock options in IXICO; holds patents on MR imaging methods. Other relationships: none to disclose.

References

1. Chen Q, Levine D. Fast fetal magnetic resonance imaging techniques. Top Magn Reson Imaging 2001;12(1):67–79.
2. Huisman TA, Martin E, Kubik-Huch R, Marincek B. Fetal magnetic resonance imaging of the brain: technical considerations and normal brain development. Eur Radiol 2002;12(8):1941–1951.
3. Huppert BJ, Brandt KR, Ramin KD, King BF. Single-shot fast spin-echo MR imaging of the fetus: a pictorial essay. RadioGraphics 1999;19(Spec Issue):S215–S227.
4. Wagenvoort AM, Bekker MN, Go AT, et al. Ultrafast scan magnetic resonance in prenatal diagnosis. Fetal Diagn Ther 2000;15(6):364–372.
5. Sandrasegaran K, Lall C, Aisen AA, Rajesh A, Cohen MD. Fast fetal magnetic resonance imaging. J Comput Assist Tomogr 2005;29(4):487–498.
6. Rutherford MA, Jiang S, Allsop JM, et al. MR imaging methods for assessing fetal brain development. Dev Neurobiol 2008;68(6):700–711.
7. Rutherford MA. Magnetic resonance imaging of the fetal brain. Curr Opin Obstet Gynecol 2009;21(2):180–186.
8. Stehling MK, Holzknecht NG, Laub G, Böhm D, von Smekal A, Reiser M. Single-shot T1- and T2-weighted magnetic resonance imaging of the heart with black blood: preliminary experience. MAGMA 1996;4(3-4):231–240.
9. Kawamitsu H, Sugimura K, Van Cauteren M. Heavily T1-weighted images without respiratory artifacts: partial angle inversion recovery fast spin-echo imaging (PAIR-FSE). J Magn Reson Imaging 2000;12(6):960–964.
10. Hajnal JV, Bryant DJ, Kasuboski L, et al. Use of fluid attenuated inversion recovery (FLAIR) pulse sequences in MRI of the brain. J Comput Assist Tomogr 1992;16(6):841–844.
11. Prayer D, Brugger PC, Prayer L. Fetal MRI: techniques and protocols. Pediatr Radiol 2004;34(9):685–693.
12. Hou P, Hasan KM, Sitton CW, Wolinsky JS, Narayana PA. Phase-sensitive T1 inversion recovery imaging: a time-efficient interleaved technique for improved tissue contrast in neuroimaging. AJNR Am J Neuroradiol 2005;26(6):1432–1438.
13. Malamateniou C, McGuinness A, Nunes R, et al. T1-weighted MRI of the fetal brain with 3D reconstruction using single shot techniques. In: Proceedings of the European Society for Magnetic Resonance in Medicine and Biology. Antalya, Turkey: European Society for Magnetic Resonance in Medicine and Biology, 2009;246.
14. Levine D. Obstetric MRI. J Magn Reson Imaging 2006;24(1):1–15.
15. Woolrich MW, Jbabdi S, Patenaude B, et al. Bayesian analysis of neuroimaging data in FSL. Neuroimage 2009;45(1 suppl):S173–S186.
16. Smith SM, Jenkinson M, Woolrich MW, et al. Advances in functional and structural MR image analysis and implementation as FSL. Neuroimage 2004;23(suppl 1):S208–S219.
17. Tello R, Crewson PE. Hypothesis testing II: means. Radiology 2003;227(1):1–4.
18. De Muth JE. Overview of biostatistics used in clinical research. Am J Health Syst Pharm 2009;66(1):70–81.
19. McCrum-Gardner E. Which is the correct statistical test to use? Br J Oral Maxillofac Surg 2008;46(1):38–41.
20. Kundel HL, Polansky M. Measurement of observer agreement. Radiology 2003;228(2):303–308.
21. Polansky M. Agreement and accuracy: mixture distribution analysis. In: Beutel J, VanMeter R, Kundel H, eds. Handbook of imaging physics and perception. Bellingham, Wash: Society of Professional Imaging Engineers, 2000; 797–835.